Forest Ecology and Management 477 (2020) 118482

Contents lists available at ScienceDirect

Forest Ecology and Management

journal homepage: www.elsevier.com/locate/foreco

The effect of the 'Las Maquinas' wildfire of 2017 on the hydrologic balance of a high conservation value Hualo (*Nothofagus glauca* (Phil.) Krasser) forest in central Chile

Francisco Balocchi[a,b,*], Neftali Flores[c], Daniel Neary[d], Don A White[e,f], Richard Silberstein[f,g,h], Pablo Ramírez de Arellano[a]

[a] *Bioforest SA, Camino a Coronel s/n km 15, Coronel, Chile*
[b] *Water Resources Department, Universidad de Concepción, Chillán, Chile*
[c] *Facultad de Ciencias Forestales, Universidad de Concepción, Concepción, Chile*
[d] *USDA Forest Service, Rocky Mountain Research Station, 2500 South Pine Knoll Drive, Flagstaff, AZ 86001, USA*
[e] *Whitegum Forest and Natural Resources Pty. Ltd., Midland, WA 6056, Australia*
[f] *Edith Cowan University, Western Australia, Australia*
[g] *Hydrological and Environmental Scientific Solutions Pty Ltd., Western Australia, Australia*
[h] *University of Western Australia, Nedlands, Western Australia, Australia*

ARTICLE INFO

Keywords:
Wildfire
Runoff coefficient
Streamflow
Groundwater
Soil storage
Transpiration

ABSTRACT

The large wildfires of January 2017 burned more than 500,000 ha, including areas of high conservation value native forest, in central Chile. Runoff, streamflow and water balance were measured in a native forest catchment for 7 years before and 2 years after the fires. The annual peak flows and runoff coefficients decreased after the fire as did summer flows and total streamflow. These reductions in flow were despite rainfall being higher in the two years after the fire than in the two years before the fire. The forest re-sprouted vigorously after the fire and evapotranspiration in the second year after the fire was approximately two thirds of the rate before the fire. While the forest water use is recovering rapidly, streamflow in the two years after the fire was reduced relative to the seven years before the fire. In the two years after the fires, more than 50% of rainfall is not accounted for by either evapotranspiration or by streamflow. Potential explanations for this gap in the water balance include recovery in storage after the fire and increased bypass flow below the measuring weirs.

1. Introduction

The largest single wildfire event in the recent history of Chile, known locally as the 'las maquinas' fires, burned more than 500,000 ha of land in Central Chile in January of 2017 (De la Barrera et al., 2018). The extent of these fires was unprecedented in the post Columbian history of Chile and caused loss of life, property and the destruction of native forest, crops and large areas of commercial plantations. The effect of these fires on forest production and natural ecosystems in the region will likely be long lasting. In the region where the fires occurred the security of water supply is also a daily concern for the local people with many dependent on local stream and well extraction. The removal of vegetation cover and the litter layer has the potential to affect catchment hydrologic processes such as interception, evaporation and transpiration, as well as infiltration rates and expose the soil more directly to the impact of rainfall (Nolan et al., 2015; Poon and Kinoshita, 2018; Shakesby and Doerr, 2006). These factors may also result in changes to baseflow, peak flow and water yield (Kinoshita and Hogue, 2011). Such fundamental changes in hydrologic processes (DeBano et al., 1998) have the potential to affect the security of water supply for local people. Quantifying and understanding these changes will therefore be very important as a basis for future forest and water management strategies in the region.

The most commonly observed pattern of evapotranspiration and streamflow after a fire may be characterised by three phases described by the Kuczera curves (Kuczera, 1987). Immediately after the fire streamflow increases for a period due primarily to a reduction in cover and evapotranspiration (Scott, 1993; Wine et al., 2018). In the second post-fire phase, as the forest cover increases, evaporation also increases and eventually streamflow is less than immediately before the fire (Jayasuriya et al., 1993). In a third phase, the forest ages and streamflow return to a pre-fire rate. In forests that regenerate after fire from

* Corresponding author at: Bioforest SA, Camino a Coronel s/n km 15, Coronel, Chile.
E-mail address: francisco.balocchi@arauco.com (F. Balocchi).

https://doi.org/10.1016/j.foreco.2020.118482
Received 24 January 2020; Received in revised form 29 July 2020; Accepted 31 July 2020

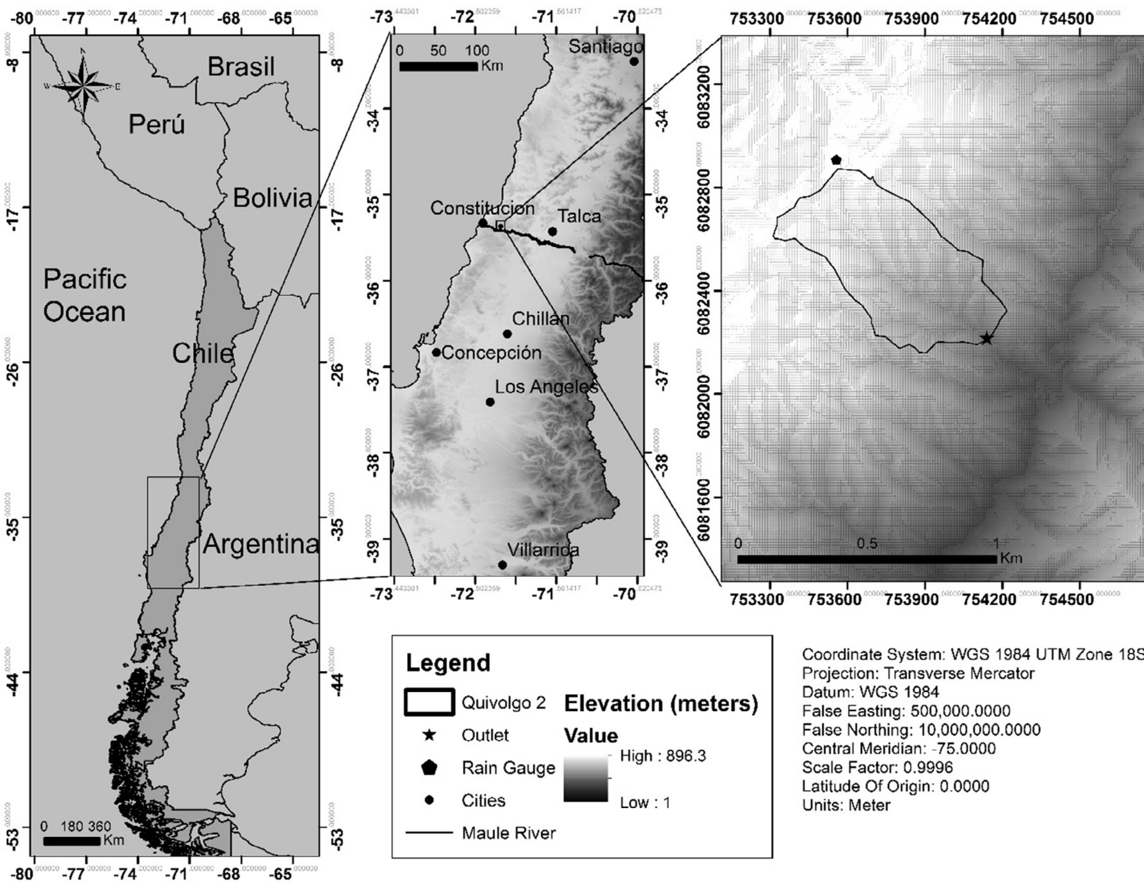

Fig. 1. The location of the weir and rain gauge within the catchment, the catchment and the important cities within Chile.

seedlings, this transition to pre-fire hydrology may take many decades (Jayasuriya et al., 1993) while forests that re-sprout from existing stems and root systems may transition through this cycle within a decade (Nolan et al., 2015). In the latter part of the twentieth century, the expectation of increased streamflow immediately after fire became an established tenet of forest hydrology (see for example, Nyman et al., 2010; Shakesby and Doerr, 2006). However, in recent times, with an increase in forest fire frequency and severity, some researchers have observed a decrease in flow after fire. For example, Feikema et al. (2013) found that changes in streamflow after a fire can be hard to detect because although the canopy is reduced, the need to replenish a severe soil moisture deficit can delay the recovery of streamflow. Nolan et al. (2015) observed a decrease in streamflow during the first four years after a fire in Australia and attributed this to a period of increase in catchment water storage. Such reductions in streamflow after fire have also been observed in Canadian (Owens et al., 2013) and Californian forested catchments (Bart and Tague, 2017).

It is noteworthy that unchanged or increased flow immediately after fire seems to have been observed in re-sprouting forests rather than those that regenerate from seedlings. In burned catchments the post-fire flow regime is the result of the combined effects of the recovery of the sapwood area index of the vegetation, changes in soil conditions caused by the fire and the capacity of the soil and groundwater to store more water. In a re-sprouting forest, such as the Hualo (*Nothofagus glauca* Phil. (Krasser)) type forest that is common in the area burned in the northern part of the coastal rage in Chile (Fajardo and Alaback, 2005) rapid recovery of sapwood area index can result in the recovery of evapotranspiration to pre-fire values within two to four years (Nolan et al., 2014; White et al., 2020).

After fire, a reduction (often 50–85%) in the rate of water infiltration into soil is often observed (Imeson et al., 1992; Moody and Ebel, 2012; Moody and Martin, 2001b). This reduction is mainly attributed to the formation of hydrophobic layers in the soil (Beatty and Smith, 2013; Ebel and Moody, 2013; Imeson et al., 1992; Moody and Ebel, 2012; Moody and Martin, 2001a; Shakesby et al., 1993; Ubeda and Sala, 1996; Varela et al., 2007) and has been observed in Chile (Garcia-Chevesich et al., 2019). The production of a fire-induced water repellence may combine with the loss of protective vegetative cover to increase runoff and erosion (Garcia-Chevesich et al., 2019; Ferreira et al., 2000; Onda et al., 2008; Sheridan et al., 2007). Other mechanisms that may reduce infiltration rates include soil sealing (e.g. Larsen et al., 2009), hyper-dry conditions (Moody and Ebel, 2012), reduction of preferential flow pathways (e.g. Nyman et al., 2014), and reductions in soil organic matter that change soil structure (e.g. Moody et al., 2016).

After a fire, a decrease in infiltration rate can have contrasting effects on the surface and sub-surface flow conditions. It enhances the overland flow by increasing the amount of precipitation that is converted to runoff. In doing so, it can lower sub-surface flow by reducing the amount of precipitation that seeps underground. In a paired-catchment analysis, Loáciga et al. (2001) observed an increase in the annual streamflow of up to 20–30% after a wildfire. Mahat et al. (2016) used a two unburned and two burned catchments to study the impact of the 2003 Lost Creek wildfire on streamflow in Alberta, Canada. They observed an increase in the annual streamflow of 20–100% in the first five years, with peak flows 40–120% greater in the burned catchment. Some authors (e.g. Lane et al., 2006) observed annual flows that were higher in the second year post-fire than in the first and that these flows were higher than expected for a post-fire disturbance in a wet eucalypt forest in south-eastern Australia.

Prior to the wildfire of 2017 in central Chile, catchment and stand scale water balance components were being measured in a native forest stand of the Hualo type forest. These measurements continued after the fire, after a break of several months. The effect of fire on the individual components of evapotranspiration was reported by White et al. (2020). In this paper we report the components of the water balance expressed at the catchment scale which is located in latitude 35.35°S; longitude 72.2°W. These data are used to test the hypothesis that wildfire will result in increased streamflow, or at least an increase in the proportion of rain that ends up in the stream, for at least two years after the fire.

2. Materials and methods

2.1. Study site

The study site (in the locality of Quivolgo) is a native forest catchment approximately 20 km north east of the city of Constitución in Central Chile in the western part of the Maule region, in the coastal range of south-central Chile (Fig. 1). The catchment (latitude 35.35°S; longitude 72.2°W) has an area of 33.03 ha, a south easterly aspect, an average slope of 27.3% and range of elevation between 305 and 526 m above sea level. The soil is very shallow, varying in depth from 0 cm to a maximum of 100 cm with a silt, clay, and sand content of 36, 40, and 24%, respectively (Clay Loam soils). It overlies fractured rocks of the Dollimo Complex of the western coastal range that was described in detail by Gana and Hervé (1983). The rocks of the region are a mix of albite schists, greenschist derived from metamorphism of oceanic tholeiitic basalts, iron and manganese rich metachaerts, serpentinites with occasional marble lenses. This shallow soil is mixed with fragments of the rock and the underlying rock is very broken and includes deep seams of partially weathered material.

The catchment has a Temperate semi-oceanic climate type, with a mean annual precipitation of 966 mm, the majority of which falls between May and September (Bravo-Linares et al., 2018). The maximum temperature in the warmest month is around 26 °C and the minimum in the coolest month is 1.3 °C. The seasonal pattern of precipitation and temperature for this catchment are shown in Fig. 2.

Average annual streamflow flow was 346 mm before the fire, and the highest yield between 2009 and 2016 was observed in 2014 (458 mm) and the lowest occurred in 2016 (223 mm). Average summer flow (January-March) was 63.7 mm before the fire. A monthly hydrograph pre- and post-fire can be found on Fig. 3.

The catchment is covered by Hualo type native forest and the dominant species on the ridges and steep slopes is the winter deciduous *Nothofagus glauca*. There are also nine evergreen species present in the overstorey, including *Aextoxicon punctatum* Ruiz & Pav. (Olivillo), *Persea lingue* Nees. (Lingue) and *Cryptocaria alba* (Mol.) Looser (Peumo)

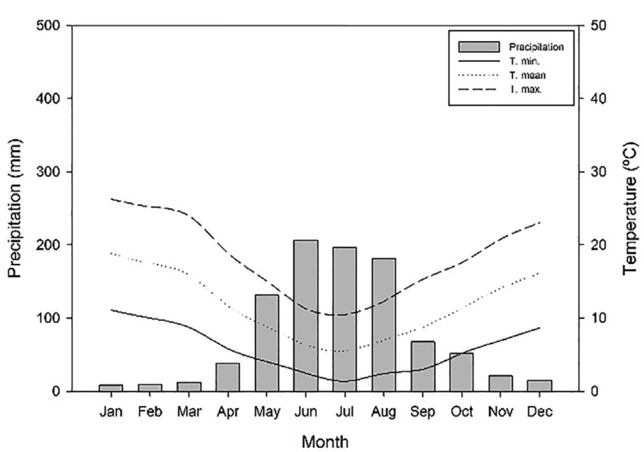

Fig. 2. Average monthly precipitation, maximum, minimum and average temperature between 2010 and 2016, the seven year period that preceded the fire.

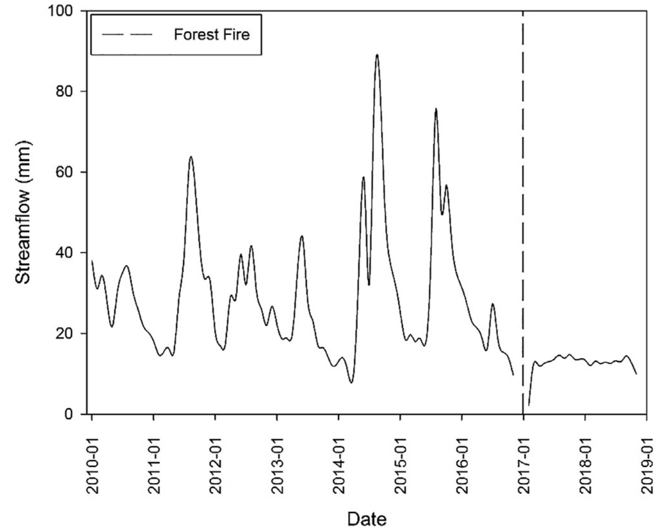

Fig. 3. Quivolgo catchment pre-and post-fire monthly streamflow 2010–2018 (mm).

which are prevalent in the drainage lines in the catchment. The structure of the forests in this catchment before and after the fires of January 2019 was described in detail by White et al. (2020).

The wildfire in January 2017, was classified as high severity using the differential Normalized Burn Ratio (dNBR) index before and after fires (De la Barrera et al., 2018). Prior to the fire the trees in the ridgetop forests of *N. glauca* had an average height of 13 m and the average basal area was 35 m^2 ha^{-1}. The evergreen stands were slightly shorter at 12 m and their basal area was 29 m^2 ha^{-1}. In March of 2019, just over two years after the fires, approximately 80% of the original *N. glauca* trees had re-sprouted from within their crowns. The average basal area of these trees was 14.5 m^2 ha^{-1}. None of the other species had grown new foliage in the crowns, although some individuals of all the species had re-sprouted at ground level. Two years after the fire, about 65% of the original stand basal area was supporting some live foliage either in the crown or at ground level. The leaf area index was nearly 5 before the fire and had recovered to approximately 3 by the end of the summer of 2019 (White et al., 2020).

2.2. Catchment scale water balance components

2.2.1. Streamflow

In 2010, a v-notch weir was installed at the outlet of the catchment and this was instrumented with a pressure transducer flow gauge (OTT, Kempten, Germany). Depth of the water in the weir was measured at 5-minute intervals and these data were used to estimate streamflow (Eli, 1986). The stream is perennial. After the fires, there is a gap in the data between January and February 2017 as it took some time to reinstall the weir and sensors after the fires. However, all years were complete from March to November. Changes in hydrologic year flows (March-November), winter (May-August), and spring (September-November) were assessed following the 2017 wildfires. In this part of Chile the lowest flow occurs in March (Ahearn, 2008) and hence data from this month was chosen to represent 'low flow' conditions in these analyses.

2.2.2. Rainfall

Rainfall was measured immediately adjacent to the top of the catchment using an RG12 tipping bucket gauge (Environdata™, Queensland, Australia - Fig. 1 for location). The measurements commenced in August 2016. For the period between 2010 and August 2016, daily rainfall was sourced from the nearby meteorological site (Forel station, Direccion General de Aguas, DGA) which is about 5 km southeast of the catchment. There was a strong linear relationship (R^2 of

0.84) between rain recorded at our gauge and the DGA gauge in Forel. This was used to fill any gaps in the data. Periods of missing data from the Forel station prior to August 2016 were filled using data from the next nearest DGA station at Nirivilo, also using a linear regression.

2.2.3. Plot scale water balance

White et al. (2020) estimated transpiration, interception and soil evaporation, basal area, sapwood area and leaf area index in plots both within the experimental catchment used here and in a fragment of native forest in an adjacent catchment. In this paper, these stand scale estimates of evapotranspiration and components are assumed to apply at the catchment scale. These data are therefore used to estimate evapotranspiration before and after the fire. The detailed methods are in White et al. (2020), a brief summary is provided here.

2.2.3.1. Transpiration. Before the fire, transpiration was estimated from heat pulse sap flow measurements made in three trees in each of five plots (three of the *N. glauca* forest, two dominated by evergreen species, see Fig. 1 and White et al. (2020) for locations of the plots and the detailed method used). These measurements were used to estimate stand transpiration as the product of average monthly sap flux density and sapwood area. Sapwood area was estimated from linear relationships between sapwood area and basal area that were in turn estimated by staining increment cores collected before and after the fire (White et al. 2020).

After the fire, the sap flow measurements were continued from January 2018 in the same trees and in the same plot near the top of the catchment. The strong linear relationship between monthly transpiration measured at studied plots and the total solar radiation measured at Forel ($r^2 > 0.8$), was used to complete a record of monthly transpiration for all plots for the year before the fire. Transpiration was assumed to be zero for the first seven months after the fire when the leaf area index was zero. A separate relationship between solar radiation, based on post-fire measurements, was used to estimate transpiration in spring and early summer of 2017 (White et al., 2020).

2.2.3.2. Interception. Before the fire, throughfall was measured in the same plots as transpiration (5 plots). After the fire, throughfall measurements continued in three of these plots. In each plot, throughfall was measured using a combination of an RG12 tipping bucket rain gauge located at the centre of the plot and five Nylex™ 1000 (Nylex Pty Ltd, Australia) plastic storage rain gauges located at the centre and 5 m from the centre on each of the four cardinal directions.

For periods with missing throughfall records, daily throughfall was estimated using the linear relationship between daily throughfall for each plot and rainfall measured outside the catchment. In this way a continuous record of interception was constructed for the year before and two years after the fire.

2.2.3.3. Soil and understorey evaporation. Records of total daily solar radiation were available from the weather station at Forel (see White et al., 2020). Before the fires, three Apogee SP-212 (Apogee, USA) pyranometers were installed beneath the canopy in three plots. After the fires, in January 2018, two sensors were installed in the same plot where measurements of sapflow were recommenced. These sensors were about 50 cm above the ground and measured radiation beneath the canopy. The missing monthly records were filled using the Forel weather station data. These data were used to estimate soil evaporation using the method described in (Ren et al., 2019). Briefly, a 'crop factor' was calculated that was a function of the soil water content at the start of the month where the soil was assumed to be 70 cm deep. This crop factor was multiplied by the equilibrium rate of evaporation estimated for below the canopy. Evapotranspiration (transpiration plus this soil evaporation estimate) was then removed from the soil to estimate the crop factor for the next month. Monthly evapotranspiration was calculated as the sum of soil evaporation, interception and transpiration and expressed on a ground area basis (White et al., 2020).

2.2.3.4. Soil water content to 1.2 m. In April and June 2017, several months after the fire, but before the first major rains of 2017, six Sentek Drill and Drop™ (Sentek Sensor Technologies, Australia) probes were installed in two plots. One of these plots was the *N. glauca* plot where the sapflow sensors were re-installed in January of 2018. The other plot was on a steep slope a short distance from the catchment measurement weir and covered with mostly evergreen species with a few individuals of *N. glauca*.

In each plot, three 1.2 m and three 0.6 m probes were installed in the soil and rock. These tapered probes were installed between four and five metres from the plot centre. They were spaced evenly in a circle around this centre. When installed so that the cable end of the probe was level with the ground, these probes have sensors every 10 cm from 5 cm below ground, thus to 55 cm in the short probes and to 115 cm in the 1.2 m probes.

A measurement of volumetric water content of the soil (θ) was recorded at each depth in each probe every hour. From these data the average soil water content was calculated for each 10 cm depth interval centred on the sensor positions (average of six measurements to 60 cm and three measurements to 120 cm) and these measurements were then integrated over the depth of the probe to give an estimate of water storage (in mm) in the top 1.2 m of soil.

The variability of the mix of rocks and soil makes it very difficult to get good measurements of absolute soil water content with any sensor, however the sensors reliably indicate changes in soil moisture content, which is our main concern. The change in storage between measurements was estimated and accumulated over the duration of the experiment to quantify the net change in storage in the soil in the catchment. The net change in soil water content in the soil profile was estimated during each year after the fire. This change, the streamflow and the evapotranspiration were calculated. The residual represents the amount of water that is unaccounted for in our water balance.

2.2.4. Analysis

2.2.4.1. Catchment scale water balance. Stream flow duration curves pre- and post-fire were built using the Weibull plotting position (Makkonen, 2006) to compare the probability of exceedance at the 25th, 50th and 95**th** percentiles. Baseflow yield was calculated using the Recursive Digital Filter passed forward, backward, and forward over the streamflow data and using a filter of 0.925 (Nathan and McMahon, 1990). Later, baseflow over total streamflow per year and per pre- and post-fire was calculated. A double mass analysis was used to compare monthly streamflow before and after the wildfire and the runoff coefficient (RC, the ratio of stream flow to rainfall) was calculated for winter (May-August), autumn–winter (April-August) and for the full year (March-November). Annual peak flow rate ($m^3 s^{-1}$) was determined for each of the seven years of record. These peak flow rates were compared with the daily rainfall immediately preceding that peak flow. Days with similar total rainfall were found before and after the fire in order to detect any change in the magnitude of the peak flow and the daily water yield from that amount of rainfall.

2.2.4.2. Stand scale. Annual transpiration, interception, soil evaporation and evapotranspiration were calculated for three plots for the year before the fire and for the two years after. A simple *t*-test was used to test for the significance of differences in the water balance between years and before and after the fire.

3. Results

3.1. Annual total flow and seasonal flow

Streamflow was analysed for the periods between March and November, both before and after the wildfire. This period was selected

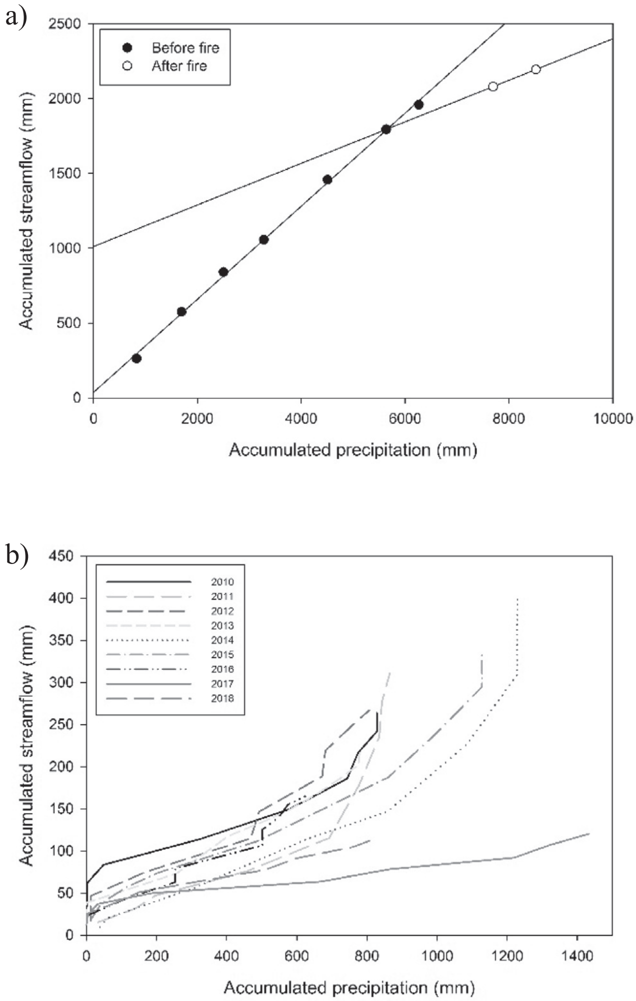

Fig. 4. March-November accumulated streamflow in Q2. a) Double mass curve of cumulative annual streamflow against cumulative annual rainfall. b) March-November cumulative streamflow against cumulative rainfall.

because the instruments and the weir were reinstalled after wildfire in February 2017 and the data record is complete for this period in every year. Using March-November data, the slope of the relationship between cumulative streamflow data and cumulative rain was much less after the fire (Fig. 4a) indicating a reduction in runoff coefficient after this fire. Additionally, total accumulated flow in 2017 was considerably lower than previous years despite more than 1464 mm of precipitation; this was 200 mm more precipitation than in 2014 but total flow was 70% less than that year. Likewise, for years with similar precipitation to 2018 (800–900 mm), total flow was significantly lower than in those years before the fire (Fig. 4b).

The pre-fire annual water yield ratio (or streamflow per unit precipitation) was higher than observed after the fire (Fig. 5a). In the seven years before the fire, the maximum and minimum total flow from March to November were, respectively, 399 mm yr^{-1} in 2014 and 164 mm yr^{-1} in 2016. (Table 1).

March-November flow during 2017, the first year after fire, when the catchment received the highest annual rainfall since 2009, was 26% less than the lowest annual flow observed prior to the fire. In 2018, March-November streamflow was 5% lower than in 2017, and this was associated with a 41% reduction in precipitation.

Similar patterns were evident in annual (March-November) and winter (May-August) streamflow and precipitation (Fig. 5b). The maximum winter flow in the seven years before the fire was observed in 2014 and the minimum occurred in 2016, which had the driest winter. In the two years after the fire, winter flows were only 54 mm yr^{-1} in 2017 and 52 mm yr^{-1} in 2018. For the seven years before the fire, the relationship between spring (September-November) streamflow and rainfall was weaker than that observed during winter or for the full year but was nonetheless statistically significant. After the fire, the spring flow was 42 mm yr^{-1} in 2017 and 37 mm yr^{-1} in 2018 (Fig. 5c).

3.2. Runoff coefficient (RC)

From 2010 to 2015 the annual runoff coefficient (RC) varied between 27% and 35% and was 26% in 2016 when the lowest annual rainfall for the pre-fire period was also observed. After the fire, the runoff coefficient decreased significantly and was 8.4% in 2017 and 14% in 2018. The temporal pattern of the autumn–winter runoff coefficient (April-August) was similar to that of the annual coefficient (March-November) although the autumn–winter and winter (May-August) RC was always less than the total annual RC. The minimum autumn–winter RC of 7.6% was observed in 2017 while the value was 12.6% in 2018. The minimum value of winter RC was observed after the fire in 2017 (6.24%) and it increased in 2018 (10.2%) (Fig. 6).

3.3. Peak flows and daily water yield

Peak flow was highly variable but, interestingly, it was lower after the fire than before, despite the much higher daily precipitation (Table 2 and Fig. 7a). The highest peak flow of 0.045 $m^3\ s^{-1}$ and daily water yield of 12.3 mm were both observed in 2014, and these peak values were associated with a daily rainfall of 48.7 mm. However, there was no relationship between daily rainfall and daily streamflow yield. For instance, a rainfall of 40.4 mm d^{-1} yielded a peak flow of 0.01 $m^3\ s^{-1}$ and daily water yield of 2.77 mm in 2016. In 2013, on the other hand, a rainfall of 105 mm d^{-1} yielded just 0.02 $m^3\ s^{-1}$ of peak flow and 5.56 mm of daily flow.

Additionally, the response of the catchment to the same rainfall intensity (30 min) was evaluated before and after the fire when possible, that is between August, when the rain gauge was installed, and December 2016. In 2016, a maximum rate of 5.6 mm h^{-1} of rainfall was measured; in this period the flow increased from 0.0026 $m^3\ s^{-1}$ to 0.0029 $m^3\ s^{-1}$ in the next half hour, reaching its maximum value after 2 h. In 2017, the same intensity (5.6 mm h^{-1}) was found, but the flow rose only from 0.00221 $m^3\ s^{-1}$ to 0.00224 $m^3\ s^{-1}$, reaching its maximum value 2 h later. Even though baseflow in 2017 was 80% of that in 2016, 2017 peak flow was just 54% of that in 2016. In 2018, on the other hand, a 5.8 mm h^{-1} was found, but increase in flow was detected with the storm period. Conversely, a delay of almost 10 h between the rainfall and the peak flow in 2018 has been identified, despite having a similar 2017 base flow. The 2018 peak flow reached only 70% of the peak identified in 2017 (Fig. 7b).

3.4. Low flows

There was a positive relationship between March flow and annual rainfall in the previous year both before and after fire. Furthermore, there was more flow in March before the fire than post-fire, with highest March flow of 34.5 mm in 2010 (following rainfall of 910 mm) and a minimum of 9.6 mm in 2014 (rainfall of 787 mm). Summer flow also declined further after the fire and was 12.4 mm in 2017 and 6.43 mm in 2019. Although summer flow was 13.1 mm in 2018, summer flows after the fire were all lower for a given rainfall than before the fire (Fig. 8).

There was a negative correlation between winter low flows and autumn–winter rainfall (coefficient of correlation −0.69) before the fire. However, after the fire this relationship was less clear. The 865 mm of rain in 2017 yielded a minimum streamflow of 0.0014 $m^3\ s^{-1}$ but when the precipitation decreased to 507 mm in 2018, the minimum streamflow only decreased a small amount to 0.0013 $m^3\ s^{-1}$ (Fig. 9).

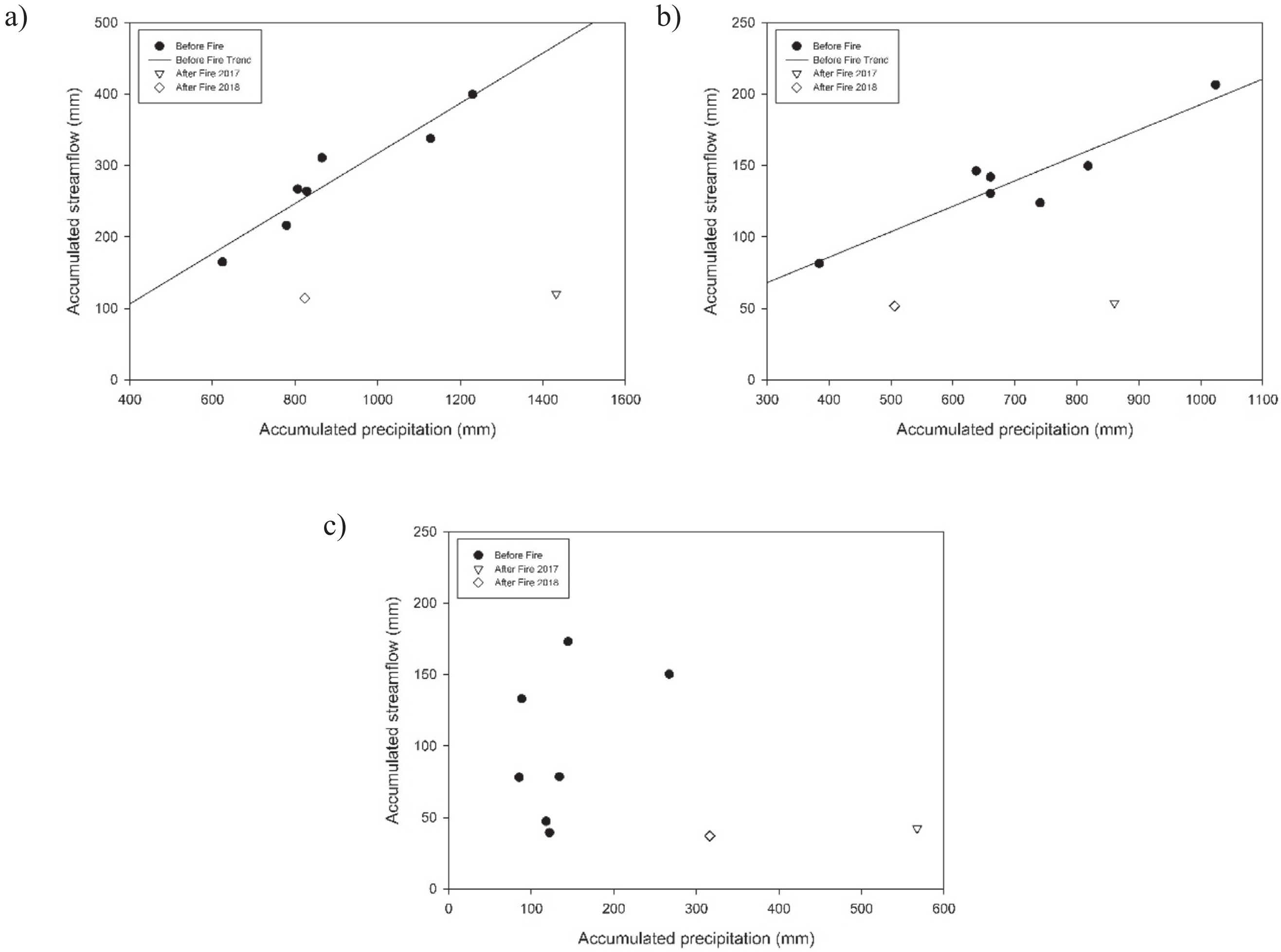

Fig. 5. Streamflow (mm) and rainfall (mm) in each year before and after the fire. Panel (a) shows the values for March-November, panel (b) shows winter rainfall and streamflow and panel (c) shows the spring values.

Table 1
Annual rainfall, annual streamflow, hydrologic year (March to November), peak flows and daily water yield before and after the fire associated with similar daily rainfall.

Year	Annual Rainfall (mm)	Total Stream flow (mm)	March to November flow (mm)
2010	860	353	263
2011	887	377	310
2012	932	331	267
2013	788	269	216
2014	1254	459	399
2015	1128	416	336
2016	686	223	164
[1]2017	1464	136	120
2018	864	148	114

[1] Instruments reinstated in February following fires in 2017.

3.5. Baseflow index (BFI)

There are similar proportions of baseflow over total flow in some years before and after fires (Table 3) such as 2013/2016 and 2017. Therefore, there exist similar proportion of baseflow before and after fires, but baseflow can be 2 times greater pre-fire. In general, pre-fire BFI was between 0.69 and 0.88 whereas post-fire was 0.93 and 0.94.

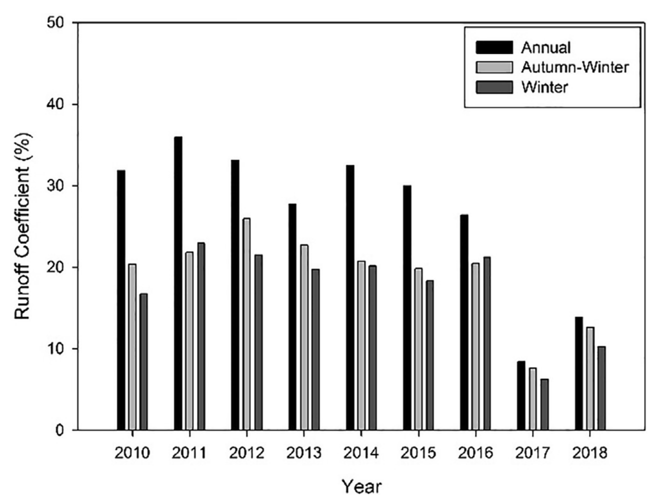

Fig. 6. The runoff coefficient (ratio of runoff to rainfall, %) before and after the fire.

3.6. Flow duration curves

The flow duration curves confirmed that the flow decreased after the fire and that decreases were evident in low and high flow. After the fire the flow associated with a 1% probability of exceedance was 7% of that observed in the years before the fire. Similar proportional

Table 2
Peak flows and daily water yield before and after the fire associated with similar daily rainfall.

Date	Peak flow (m^3 s^{-1})	*Daily water yield (mm)	**Daily precipitation (mm d^{-1})
28-Aug	0.023	6.33	54.16
14-Jul	0.033	9.07	74.84
18-Jun	0.016	4.4	38.31
28-Jun	0.02	5.56	104.97
8-Jun	0.045	12.33	43.04
6-Aug	0.043	11.93	24.46
25-Jul	0.01	2.77	40.41
25-Jun	0.0022	0.61	75.4
19-Sep	0.0041	1.29	18.37

* Total daily streamflow for that day.
** Total daily rainfall for that day.

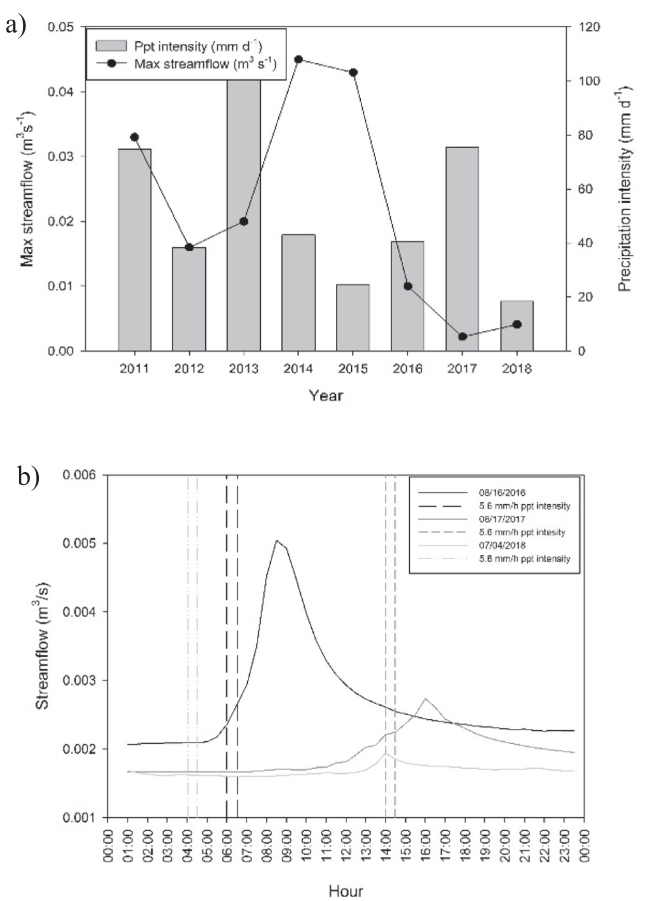

Fig. 7. Peak flows and precipitation intensity before and after fire. a) The maximum streamflow (m^3 s^{-1}) and the rainfall event that yielded that flow per day. b) Hour streamflow associated 5 mm/h intensity before (2016) and after fire (2017–2018).

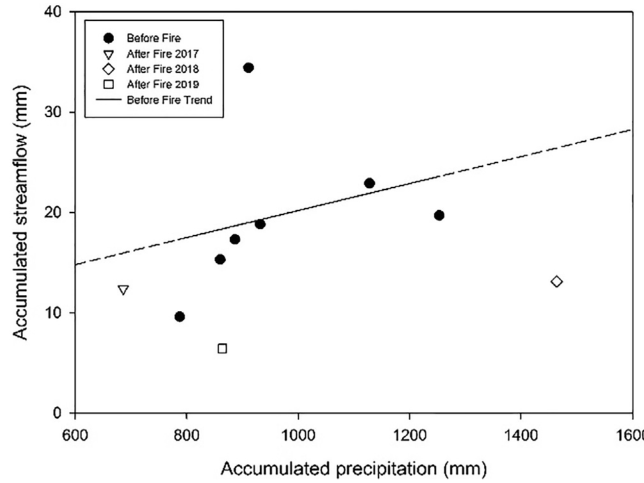

Fig. 8. March streamflow (mm) and previous year precipitation (mm) pre- and post-fire.

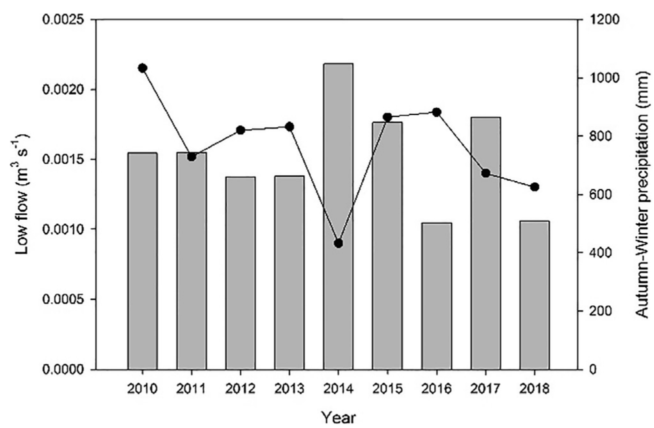

Fig. 9. Daily low flow (m^3 s^{-1}) and autumn–winter rainfall (mm), pre- and post-fire.

Table 3
Baseflow Index and baseflow yield (mm) by year before and after fires in the study site.

Year	BFI	Baseflow (mm)
2010	0.88	269.6
2011	0.77	277.4
2012	0.81	251.7
2013	0.83	202.9
2014	0.69	305.6
2015	0.83	321.7
2016	0.85	190.8
2017	0.93	127.5
2018	0.94	136.6

reductions were observed after the fire in the flows with a 25%, 50%, 95% are 38%, 54%, 40% probability of exceedance (Fig. 10).

3.7. Annual forest water balance

Annual evapotranspiration was 526 mm in the year before the fire (2016) and 323 and 355 mm in the first and second years after the (2017 and 2018, Fig. 11).

The composition of evapotranspiration also changed after the fire. In the year before the fire, transpiration (222 mm) was 32% of evapotranspiration while interception (258 mm) and soil evaporation (46 mm) contributed 49% and 9% of evapotranspiration, respectively. In the first year after the fire, transpiration (50 mm) was only 15% of evapotranspiration while the contribution of interception (145 mm) was similar at 45% and that of soil evaporation (128 mm) increased to 40%. In 2018, the second year after the fire, soil evaporation (143 mm) was still 40% of evapotranspiration, interception (85 mm) was 25% of evapotranspiration and the contribution of transpiration (127 mm) had increased to 36% (Fig. 12).

The year before the fire was drier than average (annual rainfall 686 mm), the first year after the fire was much wetter than average (1464 mm) while the annual rainfall in the second year after the fire was close to the long-term average (864 mm). In these three years, the

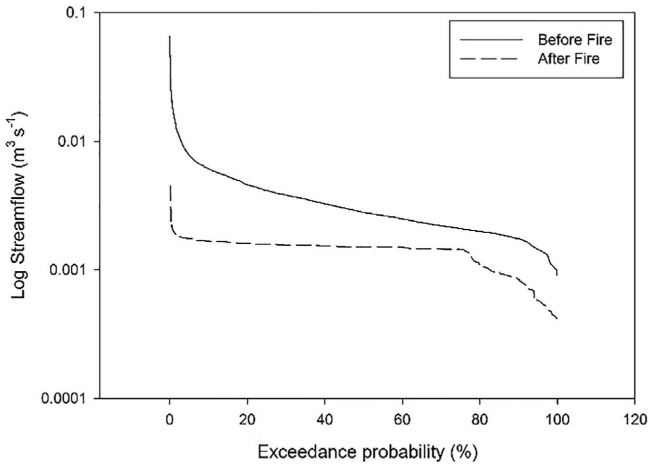

Fig. 10. Pre- and post-fire flow duration curves.

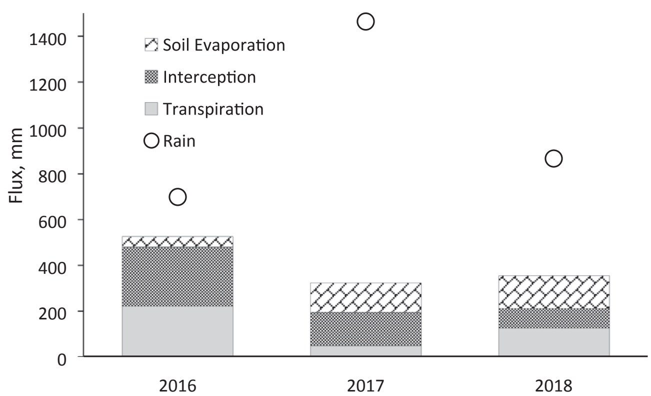

Fig. 11. Annual transpiration, interception, soil evaporation, evapotranspiration (total height of the columns) and rainfall for one year before and two years after the fires (circles).

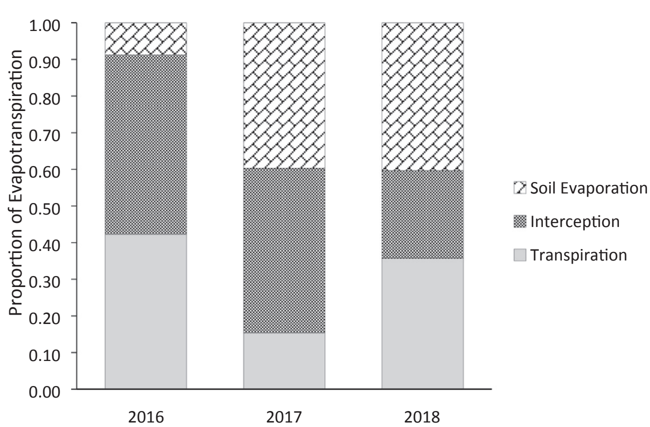

Fig. 12. Annual transpiration, interception, soil evaporation expressed as a proportion of evapotranspiration for one year before and two years after the fires.

difference between rainfall and evapotranspiration was 160 mm (2016, before the fire), 1141 mm (2017) and 509 mm (2018). In the two years after the fire the net change in soil water content was 90 mm in the first year and −60 mm in the second year (Fig. 13). The total net change was therefore about 30 mm.

After subtracting streamflow and evapotranspiration from rainfall and adding the change in storage, the net water balance in the year before the fire was −63 mm indicating a period of soil drying. In the first two years after the fire the net water balance was respectively, 915 mm and 421 mm. This means that after the fire a large amount of rainfall was not accounted for by measurements of streamflow, evapotranspiration or the change in soil water content in the top 1.2 m. (Table 4). The possible fates of this water will be considered in the discussion.

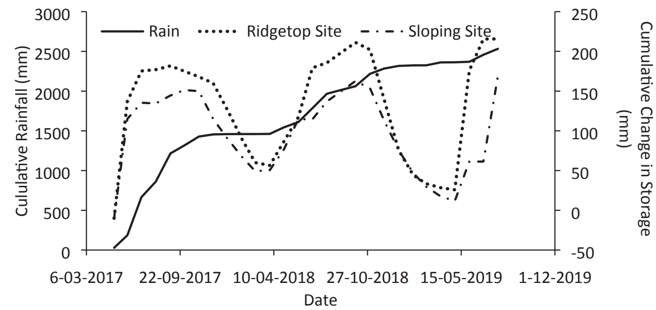

Fig. 13. Cumulative rainfall and change in soil water content in two locations in the catchment, a ridgetop location and a site on a steep slope near the weir. Data are plotted for two years after the fire.

Table 4
The water balance of this native forest catchment in the year before and the two years after the fire.

Flux (mm)	2016, Last year before fire	2017, First year after Fire	2018, Second year after fire
Rainfall	686	1464	864
Evapotranspiration	526	323	355
Change in storage	Unknown	90	−60
Streamflow	223	136	148
Net (unexplained)	−63	915	421

4. Discussion

This paper describes the total water balance of a small catchment covered with a Hualo (*N. glauca*) native forest. Perhaps the most striking finding of this paper is that, while it was possible to account for all the rainfall in the catchment before the fire, this was not possible after the fire. In the first year after the fire, evapotranspiration and streamflow both decreased, and this was associated with a doubling of rainfall relative to the year before the fire. The second year after the fire was a more 'normal' rainfall year but the sum of streamflow and evapotranspiration was still much less than rainfall. The components of this water balance are now considered in turn in the context of the international literature. The possible fates of the unexplained components of the water balance are also discussed.

The total of evapotranspiration was much less in the years after the fire than was observed in the year that preceded the fire. Interception and transpiration decreased dramatically after the fire while soil evapotranspiration increased. All these changes are, of course, entirely consistent with the loss of canopy that occurred during the fire (White et al., 2020). Nearly all the canopy was killed and removed by the fire although some dead canopy remained in the riparian zones. No living foliage remained to transpire or to intercept rainfall for up to six months after the fire. Only burned stems and branches remained. At the same time, more radiation was reaching the forest floor than before the fire and this drove an increase in soil evaporation. The reduction in evapotranspiration is as would be expected following the fire. From observations of the canopy during the third year, 2019, it would be expected that evapotranspiration will increase significantly in coming years. This will drive the recovery of the water balance in these catchments.

By the second year after the fire, transpiration had increased from

0 mm per month immediately after the fire to nearly 45 mm per month in Autumn and Spring. This was driven by rapid recovery of the crowns of the *N. glauca* and the re-sprouting from the ground level of all the other species. After fire, this forest regenerates by re-sprouting from within the crowns of the dominant *N. glauca* and from ground level in all species. It has this in common with sclerophyllous forests from Mediterranean and temperate climate zones around the world. The dry zone oak forests of Mediterranean Europe (Timbal et al., 1996) and the dry sclerophyllous eucalyptus forests (Nolan et al., 2015) on the inland slopes of the Great Dividing Range in Australia are other examples. Nolan et al. (2015) measured streamflow before and after a fire in a resprouting *Eucalyptus* forest and found that the water balance recovered to a pre-fire condition in 10–12 years after a fire. Changes in transpiration were not measured but must have occurred almost immediately as these forests, like the *N. glauca* of Chile, are known to resprout within months even after very intense wildfires (Litton and Santelices, 2002).

For the catchment water balance the reduction of evapotranspiration after the fire means that more water is potentially available to reach the streams. This did not occur. One potential fate of this water is increased water storage in the soil and in the groundwater. No measurements of groundwater depth were made in this study, but the Baseflow Index was observed to increase, indicating increased groundwater discharge as proportion of flow, even though total flow was substantially reduced. Also, some measurements of water content were made in the first 1.2 m of soil and rock. This is considered locally to be the biologically active depth of soil in these metamorphic systems. While tree roots penetrate deeper, most nutrients and water used by the trees come from this top layer. The soil was very dry at the start of the study and a cycle of wetting and drying was evident. This cycle increased in amplitude as rates of transpiration increased during the study. Two year after the fire, the trees were drying this layer almost completely each year. If the extra water is being stored in the regolith, it is in deeper layers below the active root zone. This can only have occurred if infiltration rates are high after the fire and if there is somewhere for the water to be stored.

The main tree species in the study site, *Nothofagus glauca* (Phil.) Krasser, is a deciduous species. This, coupled with a Mediterranean climate with winter dominant rainfall, means that before the fire 65% of the rain reached the forest floor and after the fire this was approximately 73% (White et al., 2020). Nevertheless, a rainfall threshold for streamflow could not be found. Peak flows and daily water yield did not show any sign of increased response to rainfall. In fact, at this stage of the catchment recovery, similar rainfall amounts are not producing peak flows as large as those observed before the fire. Given the annual rainfall in the first year after the fire (2017), this must be associated with increased infiltration and storage after the fire.

Infiltration was not measured in the catchments but after the fires there were several large rainfall events that were not associated with large surges in streamflow. It can be inferred from this that infiltration increased after the fires. This is largely at odds with previous studies of post-fire water balance where infiltration is most often reduced after fire (e.g. Ferreira et al., 2005; Moody and Martin, 2001a; Shakesby and Doerr, 2006), sometimes to as low as a half or one seventh of pre-fire levels. In a study about 15 km from this site, Garcia-Chevesich et al. (2019) found a hydrophobic layer in the topsoil of a burned *N. glauca* stand. As noted above, the WDPT (hydrophobicity, infiltration) test (DeBano, 1969, 1981) was not conducted in the Quivolgo catchment. However, the low streamflow and high baseflow index in the first year of the fire, suggests very high infiltration rates and leads to the conclusion that soils on this site did not develop an impervious layer. The fires in the region of our site were particularly severe (Forestry Governmental Institution, CONAF, 2017; De la Barrera et al., 2018). Fires of this high severity may not form hydrophobic layers. For instance, it has been found that wildfire temperatures of 270–300 °C prevent the formation of a hydrophobic layer (DeBano et al., 1976), although Ferreira et al. (2005) found that the hotter the fire the more severe the hydrophobicity.

García-Comendador et al. (2017) also found a reduction in flow delivered to a stream following fire in a terraced catchment in Mallorca, Spain. In this case, the movement of sediment in tributaries upslope resulted in water capture and increased infiltration thus reducing the water reaching the measurement station further downstream. This process may have occurred in Quivolgo but there was no terracing, and apart from observations of erosion and sediment movement occurring during storms after the fires, there was no direct evidence for this mechanism to have been active in this case.

After a fire, a number of changed soil conditions can also occur. Some, such as increased hydrophobicity, might decrease infiltration and increase flow while others including the opening of root channels might increase infiltration. The years that preceded the fires of January 2017 were unusually dry and are often referred to as the Chilean mega drought (Boisier et al., 2016), and hence the soils and catchments in the region were very dry when the fires occurred. Thus, after the fires in central Chile the low level of stored water and a rapid recovery of sapwood area would mitigate against increases in streamflow after fire.

There are several pieces of evidence in this study that point, albeit indirectly, to increased infiltration and storage in the groundwater after fire. Reduced evapotranspiration and a reduction in annual streamflow were associated with an increase in rainfall after the fire. Also, the dry season flow in the catchment was correlated with the rainfall in the previous year both before and after the fire. These results again contrast with previous studies in comparable ecosystems. Nolan et al. (2015) observed a reduction in streamflow for four years following wildfires in a re-sprouting native *Eucalyptus* forest in Australia. They suggest this is due to a rapid increase in evapotranspiration of the vegetation at least partly due the moderate intensity of the fire. At this study site, evapotranspiration was still less than the rate before the fire at least two years after the fire. Therefore, the main results suggest that the tendency of the catchment was to increase storage in the first two year after wildfire.

There are three key factors that support a hypothesis of large increases in storage as the cause of reductions in flow after the fire.

Firstly, the years preceding the fire were a series of years with lower than average rainfall. Streamflow declined steadily between 2010 and 2018 despite variation in rainfall. The cumulative rainfall in the seven years that preceded the fire was the lowest on record (Bozkurt et al., 2017). This Chilean drought would almost certainly have led to a reduction in storage in the years leading up to the fire.

Secondly, if all the water that remains unaccounted for is in storage, then the rates of infiltration in the year after the fire must have been very high. This may have been due to a combination of soil cracking during the drought and to the rapid development of burned out root channels as preferred infiltration pathways after the fire, many of which were observed in the catchment after the fires. For instance, increasing infiltration rates in burnt sites were found by Cardenas and Kanarek (2014) within a loblolly pine catchment which they related to macropore effects by burned roots. Giambastiani et al. (2018) reported this phenomenon within a coastal aquifer in Italy, and Wieting et al. (2017) did the same in Colorado, USA.

Thirdly, the metamorphic rocks of this part of the coastal range are very unusual. While the trees are only active in the top two or three metres of the soil / rock mix, the rock below the soils is not a true competent bedrock. It is made up of very fractured metamorphic rocks and the fissures in the rock contain partly weathered material. These form pathways for very deep infiltration which may have two effects. Firstly, it means that there is the potential for very large storage. Secondly, the deep recharge may have resulted in flow after the fire that bypassed the gauging station. This could only have occurred in infiltration through the surface layers increased after the fires. This is not the first paper to advance a hypothesis of increased infiltration and storage after a fire. Bart (2014) and Ruud (2019) both observed increased storage after a wildfire, either in the soil or the groundwater. Moreover, these results are consistent with those of Owens et al. (2013) in Canada who found that after a wildfire in 2004, annual flow decreased even with the increasing rainfall during that year, as did the García-Comendador et al. (2017) study.

Whatever the mechanism, the water balance in the catchment is clear. Prior to the fire, rainfall was balanced by streamflow and evapotranspiration. After the fire this was not the case and the amounts of 'surplus' water are too large to be due to normal errors associated with measurements. While some of this water would be taken up by the soil moisture deficit that had developed through the dry previous years (Feikema et al., 2013), the hypothesis here is that before the fire infiltration was blocked by a combination of filled root channels and very dry soil with high soil strength, or even an history of past fires within the zone could have built up a "natural" water repellency (Doerr et al., 2009; Rodríguez-Alleres et al., 2012). After the fire, these potential preferred pathways opened up and provided the possibility for infiltration to penetrate to the very deep fractured rock system. Under these conditions, water is able to flow to very deep layers and either be stored there or to bypass our weir. Further monitoring of the catchment, and possible installation of piezometers and deeper soil moisture sensors may help to clarify the situation.

5. Conclusions

The extensive and intense wildfires of January 2017 in Central Chile burnt more than 500,000 ha and appear to have profoundly affected the hydrologic response of this study site. The water balance measured here that is summarised in Table 4 and the analysis of annual and sub-annual streamflow characteristics before and after the fire suggest that the system has changed from a relatively simple and balanced hydrology to one in which flow has decreased in spite of an increase in rainfall and a decrease in evapotranspiration. This is unusual but is not without precedent.

This change in hydrologic response is most likely due to a change in infiltration that is associated with the removal of vegetation and opening of root channels. The unusual geology means that the rocks beneath the soil do not act as an impervious layer. Results reported here are related to soil condition and vegetation cover. In this situation, it is possible that increased infiltration after the fire has resulted in penetration of water to very deep in the system where it has either been stored or has bypassed our weirs. This requires further investigation but regardless of the explanation the hydrology of this system has changed substantially from before the recent wildfires. Continued monitoring will show whether this is a long-term or transient modification.

Author contributions

F.B. was responsible for conceptualization, data analysis and wrote the initial draft. N.F. helped to draft and edit the manuscript, data analysis, and visualization. D.N. and P.R.A. were responsible of writing—review and editing. D.W. and R.S. supervised the study and contributed to the writing, review and editing. All authors contributed to the revision and edition of the manuscript.

Funding

This research received no external funding.

CRediT authorship contribution statement

Francisco Balocchi: Conceptualization, Methodology, Writing - original draft, Investigation. **Neftali Flores:** Data curation, Writing - original draft, Visualization. **Daniel Neary:** Writing - original draft. **Don A White:** Writing - review & editing, Visualization, Supervision. **Richard Silberstein:** Writing - review & editing, Supervision. **Pablo Ramírez Arellano:** Writing - review & editing, Supervision.

Declaration of Competing Interest

The authors declare that they have no known competing financial interests or personal relationships that could have appeared to influence the work reported in this paper.

References

Ahearn, E.A., 2008. Flow durations, low-flow frequencies, and monthly median flows for selected streams in Connecticut through 2005: U.S. Geological Survey Scientific Investigations Report 2007–5270, 33 p. Available online https://pubs.usgs.gov/sir/2007/5270/ (03-05-2019).

Bart, R.R., Tague, C.L., 2017. The impact of wildfire on baseflow recession rates in California. Hydrol. Process. 31 (8), 1662–1673.

Bart, R., 2014. Regional streamflow response to wildfire in California watersheds. Doctoral thesis. San Diego State University and University of California, California, USA, June.

Beatty, S.M., Smith, J.E., 2013. Dynamic soil water repellency and infiltration in post-wildfire soils. Geoderma 192, 160–172.

Boisier, J.P., Rondanelli, R., Garreaud, R.D., Muñoz, F., 2016. Anthropogenic and natural contributions to the Southeast Pacific precipitation decline and recent megadrought in central Chile. Geophys. Res. Lett. 43 (1), 413–421.

Bozkurt, D., Rojas, M., Boisier, J.P., Valdivieso, J., 2017. Climate change impacts on hydroclimatic regimes and extremes over Andean basins in central Chile. Hydrol. Earth Syst. Sci. Discuss 1–29.

Bravo-Linares, C., Schuller, P., Castillo, A., Ovando-Fuentealba, L., Muñoz-Arcos, E., Alarcón, O., de los Santos-Villalobos, S., Cardoso, R., Muniz, M., dos Anjos, R.M., Bustamante-Ortega, R., 2018. First use of a compound-specific stable isotope (CSSI) technique to trace sediment transport in upland forest catchments of Chile. Sci. Total Environ. 618 (1114–1124), 2018. https://doi.org/10.1016/j.scitotenv.2017.09.163.

Cardenas, M.B., Kanarek, M.R., 2014. Soil moisture variation and dynamics across a wildfire burn boundary in a loblolly pine (*Pinus taeda*) forest. J. Hydrol. 519, 490–502.

CONAF, 2017. Análisis de la Afectación y Severidad de los Incendios Forestales ocurridos en enero y febrero de 2017 sobre los usos de suelo y los ecosistemas naturales presentes entre las regiones de Coquimbo y Los Ríos de Chile. Informe Técnico; Santiago, Chile, pp. 56.

DeBano, L.F. 1969. Observations on water-repellent soils in Western United States. In: DeBano, L., Letey, J., (Eds.) Proceedings of a symposium on water repellent soils. University of California: Riverside, USA, CA Davis, pp. 17–29.

DeBano, L.F., 1981. Water repellent soils: a state-of-the-art. Gen. Tech. Rep. PSW-46. Berkeley, CA: U.S. Department of Agriculture, Forest Service, Pacific Southwest Forest and Range Experiment Station. 21 p.

DeBano, L.F., Neary, D.G., Ffolliott, P.F., 1998. Fire's Effects on Ecosystems. John Wiley & Sons Inc., New York, USA, pp. 333.

DeBano, L.F., Savage, S.M., Hamilton, D.A., 1976. The transfer of heat and hydrophobic substances during burning. Soil Sci. Soc. Am. J. 40, 779–782.

De la Barrera, F., Barraza, F., Favier, P., Ruiz, V., Quense, J., 2018. Megafires in Chile 2017: Monitoring multiscale environmental impacts of burned ecosystems. Sci. Total Environ. 637–638, 1526–1536.

Doerr, S.H., Woods, S.W., Martin, D.A., Casimiro, M., 2009. 'Natural background' soil water repellency in conifer forests of the northwestern USA: its prediction and relationship to wildfire occurrence. J. Hydrol. 371 (1–4), 12–21.

Ebel, B.A., Moody, J.A., 2013. Rethinking infiltration in wildfire-affected soils. Hydrol. Process. 27, 1510–1514.

Eli, R.N., 1986. V-notch weir calibration using new parameters. J. Hydraul. Eng. 112 (4), 321–325.

Fajardo, A., Alaback, P., 2005. Effects of natural and human disturbances on the dynamics and spatial structure of *Nothofagus glauca* in south-central Chile. J. Biogeogr. 32 (10), 1811–1825.

Feikema, P.M., Sherwin, C.B., Lane, P.N.J., 2013. Influence of climate, fire severity and forest mortality on predictions of long term streamflow: potential effect of the 2009 wildfire on Melbourne's water supply catchments. J. Hydrol. 488, 1–16. https://doi.org/10.1016/j.jhydrol.2013.02.001.

Ferreira, A.J.D., Coelho, C.O.A., Boulet, A.K., Leighton-Boyce, G., Keizer, J.J., Ritsema, C.J., 2005. Influence of burning intensity on water repellency and hydrological processes at forest and shrub sites in Portugal. Aust. J. Soil Res. 43 (3), 327–336. https://doi.org/10.1071/sr04084.

Ferreira, A.J.D., Coelho, C.O.A., Walsh, R.P.D., Shakesby, R.A., Ceballos, A., Doerr, S.H., 2000. Hydrological implications of soil water-repellency in Eucalyptus globulus forests, north-central Portugal. J. Hydrol. 231, 165–177.

Gana, P., Hervé, F., 1983. Geologia del Basamento Cristalino en la Cordillera de la Costa entre los Rios Mataquito y Maule, VIII Region. Revista Geológica de Chile 19–20, 37–56. https://doi.org/10.5027/andgeoV10n2-3-a03.

Garcia-Chevesich, P., Martínez, E., García, A., Castillo, M., Garfias, R., Neary, D., Pizarro, R., Valdés, R., González, L., Venegas-Quiñones, H.L., Magni, C., 2019. Formation of post-fire water repellent layers on Nothofagus glauca (Hualo) forests, after the historical "las máquinas" wildfire in south-central Chile. Am. J. Environ. Sci. 15 (1), 1–6.

García-Comendador, J., Fortesa, J., Calsamiglia, A., Calvo-Cases, A., Estrany, J., 2017. Post-fire hydrological response and suspended sediment transport of a terraced

Mediterranean catchment. Earth Surf. Process. Landforms. https://doi.org/10.1002/esp.4181.
Giambastiani, B.M., Greggio, N., Nobili, G., Dinelli, E., Antonellini, M., 2018. Forest fire effects on groundwater in a coastal aquifer (Ravenna, Italy). Hydrol. Process. 32 (15), 2377–2389.
Imeson, A.C., Verstraten, J.M., Mulligen, E.J., Sevink, J., 1992. The effects of fire and water repellency on infiltration and runoff under mediterranean type forest. Catena 19, 345–361.
Jayasuriya, M.D.A., Dunn, G., Benyon, R., O'Shaughnessy, P.J., 1993. Some factors affecting water yield from mountain ash (*Eucalyptus regnans*) dominated forests in south-east Australia. J. Hydrol. 150, 345–367.
Kinoshita, A.M., Hogue, T.S., 2011. Spatial and temporal controls on post-fire hydrologic recovery in Southern California watersheds. Catena 87 (2), 240–252.
Kuczera, G., 1987. Prediction of water yield reductions following a bushfire in ash-mixed species eucalypt forest. J. Hydrol. 94 (3), 215–236.
Lane, P.N., Sheridan, G.J., Noske, P.J., 2006. Changes in sediments loads and discharge from small mountain catchments following wildfire in south eastern Australia. J. Hydrol. 331, 495–510.
Larsen, I.J., MacDonald, L.H., Brown, E., Rough, D., Welsh, M.J., Pietraszek, J.H., Libohova, Z., Benavides-Solorio, J.D., Schaffrath, K., 2009. Causes of post-fire runoff and erosion: water repellency, cover, or soil sealing? Soil Sci. Soc. Am. J. 73 (4), 1393–1407.
Litton, C.M., Santelices, R., 2002. Early post-fire succession in a Nothofagus glauca forest in the Coastal Cordillera of south-central Chile. Int. J. Wildland Fire 11, 115–125.
Loáciga, H.A., Pedreros, D., Roberts, D., 2001. Wildfire-streamflow interactions in a chaparral watershed. Adv. Environ. Res. 5, 295–305.
Mahat, V., Silins, U., Anderson, A., 2016. Effects of wildfire on the catchment hydrology in southwest Alberta. Catena 147, 51–60.
Makkonen, L., 2006. Plotting positions in extreme value analysis. J. Appl. Meteorol. Clim. 45, 334–340.
Moody, J.A., Ebel, B.A., Nyman, P., Martin, D.A., Stoof, C., McKinley, R., 2016. Relations between soil hydraulic properties and burn severity. Int. J. Wildland Fire 25 (3), 279–293.
Moody, J.A., Ebel, B.A., 2012. Hyper-dry conditions provide new insights into the cause of extreme floods after wildfire John. Catena 93, 58–63.
Moody, J.A., Martin, D.A., 2001a. Initial hydrologic and geomorphic response following a wildfire in the Colorado front range. Earth Surf. Process. Landforms 26, 1049–1070.
Moody, J.A., Martin, D.A., 2001b. Post-fire, rainfall intensity–peak discharge relations for three mountainous watersheds in the western USA. Hydrol. Process. 15 (15), 2981–2993.
Nathan, R.J., McMahon, T.A., 1990. Evaluation of automated techniques for base flow and recession analyses. Water Resour. Res. 26 (7), 1465–1473.
Nolan, R.H., Mitchell, P.J., Bradstock, R.A., Lane, P.N.J., 2014. Structural adjustments in resprouting trees drive differences in post-fire transpiration. Tree Physiol. 34 (2), 123–136.
Nolan, R.H., Lane, P.N., Benyon, R.G., Bradstock, R.A., Mitchell, P.J., 2015. Trends in evapotranspiration and streamflow following wildfire in resprouting eucalypt forests. J. Hydrol. 524, 614–624.
Nyman, P., Sheridan, G., Lane, P.N.J., 2010. Synergistic effects of water repellency and macropore flow on the hydraulic conductivity of a burned forest soil, south-east Australia. Hydrol. Process. 24 (20), 2871–2887. https://doi.org/10.1002/hyp.7701.
Nyman, P., Sheridan, G.J., Smith, H.G., Lane, P.N., 2014. Modeling the effects of surface storage, macropore flow and water repellency on infiltration after wildfire. J. Hydrol. 513, 301–313.
Onda, Y., Dietrich, W.E., Booker, F., 2008. Evolution of overland flow after a severe forest fire, Point Reyes, California. Catena 72 (1), 13–20.
Owens, P.N., Giles, T.R., Petticrew, E.L., Leggat, M.S., Moore, R.D., Eaton, B.C., 2013. Muted responses of streamflow and suspended sediment flux in a wildfire-affected watershed. Geomorphology 202, 128–139.
Poon, P.K., Kinoshita, A.M., 2018. Spatial and temporal evapotranspiration trends after wildfire in semi-arid landscapes Patrick K. J. Hydrol 559, 71–83.
Ren, S., White, D.A., Xiang, D., Short, T.M., Xiao, W., Chen, J., 2019. Simple model of evapotranspiration by Eucalyptus plantations for data poor areas and tested using water balance data from a small catchment in Guangxi, China. Austral. For. 1–14.
Rodríguez-Alleres, M., Varela, M.E., Benito, E., 2012. Natural severity of water repellency in pine forest soils from NW Spain and influence of wildfire severity on its persistence. Geoderma 191, 125–131.
Ruud, D., 2019. The Effects of Wildfire on Soil Hydraulic Properties in an Appalachian Hardwood Forest. Honors Bachelor of Science, Oregon State University, USA.
Scott, D.F., 1993. The hydrological effects of fire in South African mountain catchments. J. Hydrol. 150, 409–432.
Shakesby, R.A., Doerr, S.H., 2006. Wildfire as a hydrological and geomorphological agent. Earth-Sci. Rev. 74, 269–307.
Shakesby, R.A., Coelho, C.A., Ferreira, A.D., Terry, J.P., Walsh, R.P., 1993. Wildfire impacts on soil erosion and hydrology in wet mediterranean forest, Portugal. Int. J. WildIand Fire 3 (2), 95–110.
Sheridan, G.J., Lane, P.N., Noske, P.J., 2007. Quantification of hillslope runoff and erosion processes before and after wildfire in a wet Eucalyptus forest. J. Hydrol. 343 (1–2), 12–28.
Timbal, J., Aussenac, G., 1996. An overview of ecology and silviculture of indigenous oaks in France. Annales Des Sciences Forestieres 53 (2–3), 649–661.
Ubeda, X.; Sala, M. 1996. Cambios en la física de suelo e incremento de la escorrentía y la erosión tras un incendio forestal. In: Grandal, A., Pages, J., (Eds.) IV Reunión de Geomorfología, O Castro, España. Sociedad española de Geomorfología: España, pp. 559–572.
Varela, M.E., Rodríguez, M., Benito, E., 2007. Impacto del fuego en la degradación física de dos suelos forestales en Galicia. Cad. Lab. Xeol. Laxe. 32, 103–110.
White, D.A., Balocchi, F., Silberstein, R.P., de Arellano, Ramirez, Donoso, P.I., 2020. The effect of wildfire on the structure and water balance of a high conservation value Hualo (Nothofagus glauca (Phil.) Krasser) forest in central Chile. For. Ecol. Manage. 47, 118219.
Wieting, C., Ebel, B.A., Singha, K., 2017. Quantifying the effects of wildfire on changes in soil properties by surface burning of soils from the Boulder Creek Critical Zone Observatory. J. Hydrol.: Reg. Stud. 13, 43–57. https://doi.org/10.1016/j.ejrh.2017.07.006.
Wine, M.L., Cadol, D., Makhnin, O., 2018. In ecoregions across western USA streamflow increases during post-wildfire recovery. Environ. Res. Lett. 13 (1), 014010.